

Metallic mean quasicrystals and their topological invariants

Anuradha Jagannathan

Laboratoire de Physique des Solides, Université Paris-Saclay, 91405 Orsay, France

(Dated:)

Topological invariants govern many important physical properties in condensed matter systems. In this work, we obtain the complete set of topological invariants for a family of one-dimensional quasicrystals. The first and best-studied member of the family is the Fibonacci chain, while the successive ones are known in the literature as silver, bronze... and collectively as the metallic mean chains. By considering rational approximants, and by making use of the relationship between these chains and two dimensional Quantum Hall problems, we write down a gap labeling scheme for finite systems, and extend it to the quasiperiodic limit. We show, by numerical computations on open chains, that the proposed scheme correctly yields the winding numbers of edge states in each of the gaps, in all of the quasicrystals. In the strict 1D limit, we discuss properties of a simplified Hofstadter “butterfly” diagram, with the analogues of Landau levels appearing in the asymptotic limit.

I. INTRODUCTION

Topological invariants, especially those which govern physical properties are justifiably of great interest in condensed matter systems. In recent years, many studies have focused on the intrinsic topological properties of quasicrystals, and on their relation to higher dimensional periodic models. The connection between 2D quantum Hall (QH) problems and 1D quasicrystals have been pointed out in a number of early works of Bellissard and collaborators [1]. More recently, on the theoretical front, connections between 2D and 1D problems have been discussed in a projected branes approach [2] and via the Fibonacci-Hall model [3]. The latter provides a convenient platform to confirm the ideas of topological equivalence between the quasicrystal and the Harper models that underlies experimental studies in optical waveguides [4, 5]. In other experiments, edge states and associated topological invariants have been observed in Fibonacci chains of polaritonic resonators [6, 7]. Our aim in this paper is to generalize results for topological invariants to all of the members of a class of 1D quasicrystals called the “metallic mean” chains, thus providing a global description of topological invariants for an entire family of quasiperiodic structures.

Given the importance of topological properties for applications, it is of interest to understand quasicrystalline systems in particular since they are less studied compared to crystalline systems. This work gives a unified view of the topological invariants of an entire family of quasicrystals, and in doing so, marks a step forward in the understanding of quasiperiodic systems.

Our approach defines a 2D QH problem for each of the finite periodic approximants of these quasicrystals. The complete set of 2D problems corresponds to a subset of the Hofstadter butterfly diagram. These 2D models are used to write down a topological indexing ansatz for the family of quasiperiodic systems. To check the ansatz, we examine the winding of the edge states within each of the gaps, for finite open chains. The quasiperiodic limit is found as the size of the approximant is sent to infinity for all of the chains.

II. THE METALLIC MEAN QUASICRYSTALS AND THEIR APPROXIMANTS

The Fibonacci quasicrystal has lesser-known relatives going by the names of the silver mean and bronze mean quasicrystals, and so on. Electronic properties of these 1D systems – spectra, wavefunctions and wavepacket diffusion have been studied [8–10]. However, their topological characteristics have not so far been studied to our knowledge. Each of the metallic mean chains can be described in terms of an irrational number, ω_n , the largest root of the equation $\omega^2 = n\omega + 1$. For $n = 1$ this yields the golden mean, $\omega_1 = \frac{\sqrt{5}+1}{2}$, giving rise to the Fibonacci chain. The cases $n = 2$ and $n = 3$ correspond to the so-called silver and bronze means respectively.

For the n th member of the family, the infinite quasicrystal can be generated using substitution rules for the A-tile and the B-tile as follows:

$$\begin{aligned} B &\rightarrow A \\ A &\rightarrow A^n B \end{aligned} \tag{1}$$

For example, in the case $n = 2$, the substitution rules applied to an initial “seed” B yield a series of finite chains as follows: $B \rightarrow A \rightarrow AAB \rightarrow AABAABA \rightarrow AABAABAAABAABAAAB \rightarrow \dots$. The finite chains \mathcal{C}_k^n are termed approximants. The n th metallic mean quasicrystal is obtained from the series \mathcal{C}_k^n in the limit $k \rightarrow \infty$.

The substitution matrix, M , relates the number of each type of tile before and after a substitution. Defining the vector $V^{(k)} = (N_B^{(k)}, N_A^{(k)})$ where $N_{B(A)}^{(k)}$ are the number of B(A) tiles respectively, one has $V^{(k)} = MV^{(k-1)}$, with

$$M = \begin{pmatrix} 0 & 1 \\ 1 & n \end{pmatrix} \quad (2)$$

The eigenvalues of M are ω_n and ω_n^{-1} , where $\omega_n = (n + \sqrt{n^2 + 4})/2$. The Perron-Frobenius eigenvalue governs the rate of growth of the approximant chains as a function of k . That is, the number of tiles in the k th chain grows asymptotically as ω_n^k . The corresponding eigenvector gives the ratio of B tiles and A tiles in the limit $k \rightarrow \infty$. One finds $N_B^{(k)} : N_A^{(k)}$ is equal to $1 : \omega_n$, in other words, the series of chains tends towards the periodic chain. The matrices M describe Pisot systems – that is, the modulus of one eigenvalue is greater than 1, the other less than 1. This property ensures that structure fluctuations are bounded in the infinite chain [11] – indeed, quasicrystals, like crystals, are hyperuniform structures [12, 13]. This is not the case for substitutions such as $B \rightarrow AB \rightarrow B^nA$. The eigenvalues have a continued fraction expansion given by $\omega_n = [n; n, n, n, \dots]$. Truncating the continued fraction at the k th order yields rational approximants of ω_n . One has

$$\omega_n^{-1} = \lim_{k \rightarrow \infty} \omega_{n,k}^{-1}; \quad \omega_{n,k}^{-1} = \frac{P_n^{(k-1)}}{P_n^{(k)}} \quad (3)$$

where the numbers $P_n^{(k)}$ satisfy the recursion relation

$$P_n^{(k)} = nP_n^{(k-1)} + P_n^{(k-2)} \quad P_n^{(0)} = 0; P_n^{(1)} = 1 \quad (4)$$

For $n = 1$, the $P_1^{(k)}$ are the Fibonacci numbers. For $n = 2$, the $P_2^{(k)}$, are known as the Pell numbers, and the ratio $P_2^{(k+1)}/P_2^{(k)}$ tends to the silver mean $\omega_2 = (\sqrt{2} + 1)/2$ as $k \rightarrow \infty$. Similar relations hold for the other metallic means.

It will be convenient to introduce another set of numbers, $Q_n^{(k)}$. These satisfy the same recursion relation given in Eq.4 for the $P_n^{(k)}$, but the initial conditions are different, $Q_n^{(0)} = Q_n^{(1)} = 1$. The P and Q series are related by

$$Q_n^{(k)} = P_n^{(k)} + P_n^{(k-1)} \quad (5)$$

The P and Q series are distinct, except for the Fibonacci case $n = 1$. The $Q_n^{(k)}$ correspond to the number of letters in the k th approximant chain of the n th quasicrystal.

To build the 2D models of the next section, we use an alternative method of generating the metallic mean chains by the cut-and-project method starting from the 2D square lattice. The method has been described in detail elsewhere (see for example [14]), so we will be very brief. Consider a given value of n . To obtain the k th approximant, an infinite strip of rational slope $P_n^{(k-2)}/P_n^{(k-1)}$ is drawn, such that the width of the strip corresponds to a unit cell of the lattice. The approximant chain is obtained by projecting the points lying within the strip onto a line. The nearest neighbor distances along the resulting 1D chain are A (long) or B (short), and occur in a sequence which repeats periodically. The unit cell comprises $Q_n^{(k)}$ sites. We note that choosing different positions for the selection strip does not result in a new approximant for an infinite sample. In contrast, for a finite sample, shifting the selection strip results in different finite chains. This fact is relevant later on, when we consider edge states for systems with open boundary conditions.

III. TIGHT-BINDING HAMILTONIANS IN 1D AND 2D AND TOPOLOGICAL INVARIANTS

We consider hopping Hamiltonians on approximants of the metallic chain of degree n and generation k having the form

$$H^{1D}(n, k) = \sum_i t_i (c_i^\dagger c_{i+1} + h.c.) \quad (6)$$

where the summation is over site indices $i = 1, \dots$. Hopping amplitudes can take the values t_A or t_B , according to the sequence of A and B in a given approximant \mathcal{C}_k^n . The spectrum of the Hamiltonian in Eq.6 is symmetric around $E = 0$ due to the chiral symmetry present in the model. To compute topological numbers, we will proceed according to the scheme given in [3], linking the 1D Fibonacci chain to a 2D Quantum Hall problem. The 2D model describes

electrons hopping on a square lattice submitted to a fictitious “geometric flux” whose value is imposed by the slope of the selection strip. For our metallic mean approximants, this geometric flux is chosen to be

$$\phi_n^{(k)} = \frac{P_n^{(k)}}{Q_n^{(k)}}, \quad (7)$$

in units of the flux quantum ϕ_0 . The symmetry of the Hofstadter problem under $\phi \rightarrow 1 - \phi$ implies that an equivalent choice for the geometric flux is $\phi_n^{(k)} = P_n^{(k-1)}/Q_n^{(k)}$. Just as in the original QH problem [15], it is convenient to work in the Landau gauge and take the fictitious vector potential parallel to the y axis. The 2D quantum Hall problem is then described by the Hamiltonian

$$H^{2D}(\phi_n^{(k)}) = \sum_{l,m} t_{l,m}^y (c_{l,m}^\dagger c_{l,m+1} + h.c.) + t_{lm}^x (c_{l,m}^\dagger c_{l+1,m} + h.c.) \quad (8)$$

where sites are labeled according to their positions $\vec{r}_{lm} = la\vec{x} + ma\vec{y}$, where a is the lattice constant. The hopping amplitudes along vertical bonds $t_{lm}^y = t_B \exp(2\pi i l \phi_n^{(k)})$ depend on the position, while the hopping amplitudes along horizontal bonds $t^x = t_A$ are independent of the flux. In the case of isotropic hopping, $t_B = t_A = t$.

Arguments presented in [3] for the golden mean quasicrystal, and which we will not reproduce here, show that there is adiabatic continuity going from the isotropic 2D QH model to the 1D quasiperiodically modulated (with $t_B \neq t_A$) 1D system. The passage from 2D to 1D is achieved in two stages: i) starting with the isotropic 2D QH problem one progressively transforms the system into a set of parallel chains of approximants, and ii) then increasing $t_B - t_A$ from 0 to its final value. Adiabatic continuity does not hold if the dimensional reduction from 2D to 1D is carried out with $t_A \neq t_B$ (as one can show by computations of topological markers using a spectral localizer formalism [16]).

The link between the 2D and 1D problems means that topological invariants obtained for the 2DQH model carry over to the 1D metallic mean chains by adiabatic continuity. Below, our computations of topological invariants will be carried out in the 2D model.

Our labeling scheme for the gaps of the k th approximant of the n th metallic mean chain can now be given. The integrated density of states in each of the gaps, $I(j)$, equal to the fraction of states lying below the j th gap, $0 \leq I \leq 1$, can be written as

$$I_n(j) = p_j + q_j \frac{P_n^{(k)}}{Q_n^{(k)}} \quad (9)$$

where p_j and q_j are integers called gap labels, with $|q_j| \leq N/2$. This Diophantine equation Eq.9 is one of the principal results of the paper, and can be solved to determine the set of p_j and q_j for each of the gaps, $j = 1, \dots, N-1$. One would obtain the same gap labels q upto a sign change by using the complementary indexing $I_n(j) = p_j + q_j \frac{P_n^{(k-1)}}{Q_n^{(k)}}$. The index q_j is sufficient to classify a gap since the index p_j is then fixed by the condition $0 \leq I \leq 1$. Since indexation in finite systems is not unique, we will present numerical evidence below that Eq.9 correctly gives the edge state winding numbers.

In Fig.1 energy spectra for the 2D model are plotted for the first three values of n corresponding to gold, silver and bronze means. For clarity, the approximants shown are small enough, so that bands and gaps can be distinguished. The flux values are $\frac{8}{13}$, $\frac{5}{7}$ and $\frac{10}{13}$. Energy is expressed in units of t . The values of gap labels are indicated in each of the gaps. As the figures show, gap labels do not follow a simple ordering for small n (we will see below a simplification for n large). For the $n = 1$ case, the $q = \pm 1$ gap is largest for all of the approximants. It has been observed, for the Fibonacci model, that gap widths tend to decrease with increasing index q , although the behavior is not monotonic [17]. When moving up the hierarchy of approximants, the gap labels stabilize increases. The IDOS in any given gap tends to a fixed value as k is increased, with

$$\begin{aligned} I_n(q) &= \lim_{k \rightarrow \infty} I(p_j, q_j) \\ I_n(q) &= \text{Mod}[q \frac{\omega_n}{1 + \omega_n}, 1] \end{aligned} \quad (10)$$

That is, for n fixed, p and q for a given gap do not change as the size of the approximant is increased. This statement holds for the gaps which are termed stable, while the so-called transient gaps disappear for larger k [17]. The limiting case of the quasicrystal is thus seen, as expected, to be described by the gap labeling theorem [18].

The bi-infinite set of indices n and k , $k = 1, \dots, \infty$ for $n = 1, \dots, \infty$, defines a subset of the fractal Hofstadter butterfly diagram. The labeling of the gaps of the spectra has a complex structure. However, as n becomes very large, the relations Eq.4,5 and 9 together imply that the labeling becomes progressively simpler. Most of the energy

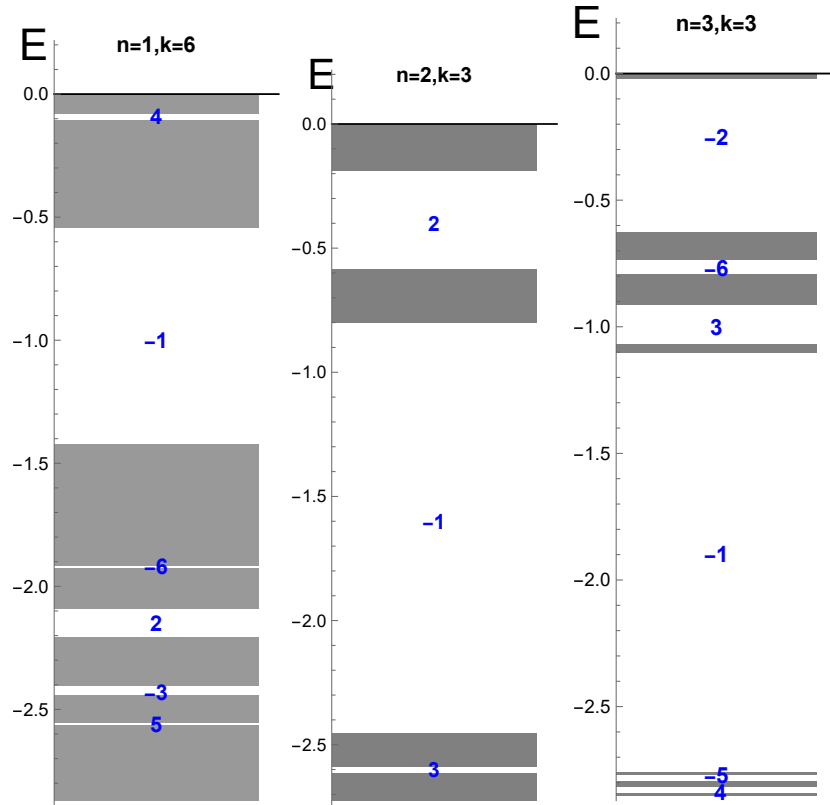


FIG. 1. The energy spectra E (in units of t) of the first three metallic mean chains, for small k (values of n and k as indicated in each figure). Bands are shown in grey, gaps in white. The absolute values of the gap index are indicated in blue within each of the gaps. For reasons of symmetry only the lower half of the spectrum is shown.

levels group together to form n bands, with each band consisting of a fraction P_{n-1}/Q_n levels. The fraction of levels not concerned by this grouping tends to zero as $P_{n-1}/Q_n \sim 1/n$. One thus obtains an indexation of the gaps that increases systematically in absolute value $-1, 2, 3, \dots$ starting from the band bottom. This is the expected small field behavior in the Hofstadter problem, where one finds Landau levels which are exactly equidistant, equidegenerate, and gap labeling of gaps occurs in a consecutive way. This simple limiting behavior of the metallic mean chains is the consequence of their having very large regions of A-bonds, separated by a single B bond, in the limit of large n .

IV. BACK TO THE 1D MODELS

The structure of the spectra of the 1D metallic mean quasicrystals is topologically equivalent to that of the Quantum Hall problem. Thus, a Hofstadter butterfly-like diagram is obtained upon plotting the spectra versus $\Omega_n = (1 + \omega_n)^{-1}$ and $\Omega_n = 1 - (1 + \omega_n)^{-1}$ respectively for the left and the right sides of the butterfly. This is shown in Fig.2. To avoid clutter we do not show approximants. The spectrum for each value of n is a Cantor set, however, numerically, one can see the principal gap structures in the butterfly by considering sufficiently large approximants. The figure has been plotted for parameters $t_A = t, t_B = 0.25t$, for values of $n = 1$ to $n = 40$, with periodic boundary conditions. Energies are in units of t . The upper and lower band edges have been outlined. One sees that the total band widths increase with n , and tend to the value 2 as $n \rightarrow \infty$, as expected for the limiting case of a chain of hoppings $t = 1$.

The main gaps of the spectrum, are shown outlined in red (for $q = \pm 1$), blue (corresponding to $q = \pm 2$) and green (corresponding to $q = \pm 3$). As n is increased by one, one sees that the ordering of gap labels is changed – for example, the gap $q = 2$ goes above the gap $q = -1$ when going from the golden to the silver mean chain. It is easy to find the values of n for which crossing of labels occur: for example, for small n , gap label 2 lies above gap label 3 (as in our examples shown in Figs.2), but their places are switched for n large enough, and such that

$$\min[I_n(q = 2), I_n(q = -2)] < \min[I_n(q = 3), I_n(q = -3)] \quad (11)$$

Using the relation for I of Eq.11 this gives the “label-crossing” to occur between $n = 3$ and $n = 4$. Other crossings

can be similarly located.

As mentioned in the previous section, the ordering of the labels becomes extremely simple for $n \rightarrow \infty$. Like the Hofstadter butterfly, where Landau levels can be seen in the corners, here too, the analogues of Landau levels can be seen at the corners of the butterfly, with groups of levels forming narrow bands, whose energies increase linearly for small Ω , with quantized slopes increasing as $q + \frac{1}{2}$.

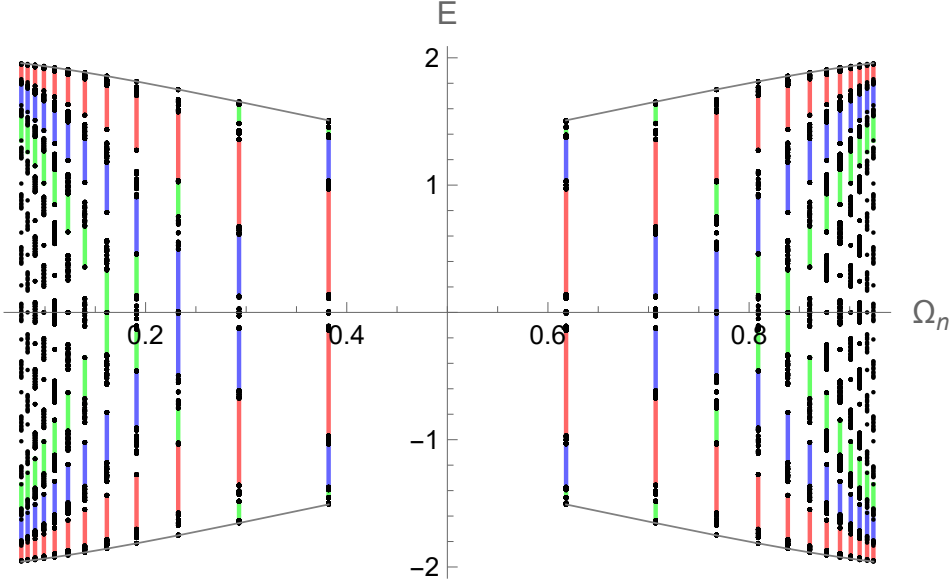


FIG. 2. A Hofstadter ‘‘butterfly’’ diagram for the 1D hopping models of the metallic mean chains Eq.8. The energy spectra for several metallic mean chains (between $n = 1$ and $n = 40$) are plotted against Ω_n (see text for definition). Each of the individual spectra (series of vertical dots) are Cantor sets in the limit $k \rightarrow \infty$, but for this figure, they were numerically computed for large approximants, with $t_A = 1, t_B = 0.25$, under periodic boundary conditions. Band edges are outlined in grey, and the four main gaps $q = \pm 1$ are outlined in red. At the corners, levels group into levels which evolve linearly as a function of flux, like the Landau levels of the Hofstadter butterfly.

V. EDGE STATE WINDING IN 1D METALLIC MEAN CHAINS

As mentioned in the previous section, the gap labeling scheme for finite chains in Eq.9 will be checked by inspecting the behavior of edge states in open chains. According to the bulk-edge correspondence principle, one should expect topological edge states. These must exhibit a winding property of the edge states as a function of the so-called phason angle, θ . The phason angle is a hidden degree of freedom of the quasicrystal system which is best visualized in the 2D representation as a displacement of the selection strip in the direction y' perpendicular to the physical axis x' . For an approximant chain of N sites, progressively shifting the selection window results in N different chains, each one differing from the previous chain by one local permutation of bonds. The initial chain is recovered at the end of the cycle. During the phason cycle, the edge states in gaps shift in energy and position. As a function of the phason angle, edge modes can jump across the chain, giving rise to topological charge transport. These changes have been observed experimentally in photonic waveguides [5] and in polaritonic resonators [7]. The relation between winding of edge states and the topological invariants of the bulk, or bulk edge correspondence which was empirically observed in experiments has been given a theoretical foundation in [19].

Fig.3 shows the energy bands and edge state energies in each of the main gaps as a function of the phason angle (for a definition of this angle see [20]) for a $N = 17$ silver mean approximant. Since the spectrum is symmetric, only the lower half of the spectrum is shown. The curves shown are not continuous, because the spectrum is only computed for a discrete number of values of θ (equal to the number of sites, 17), we have joined those data points. The ‘‘oscillations’’ of the gap state energies are irregular, although one can see that they lead to the expected value of winding number q for each gap. Indeed, one should note that an improved method by Kellendonk and Scaglioli uses a technique of ‘‘augmentation’’ of the model that smooths the ‘‘jumpy’’ behavior of edge state energies [21] and it would be interesting to apply their method to this problem.

We compare now the winding numbers deduced from Fig.3 against the gap labels obtained using the indexing

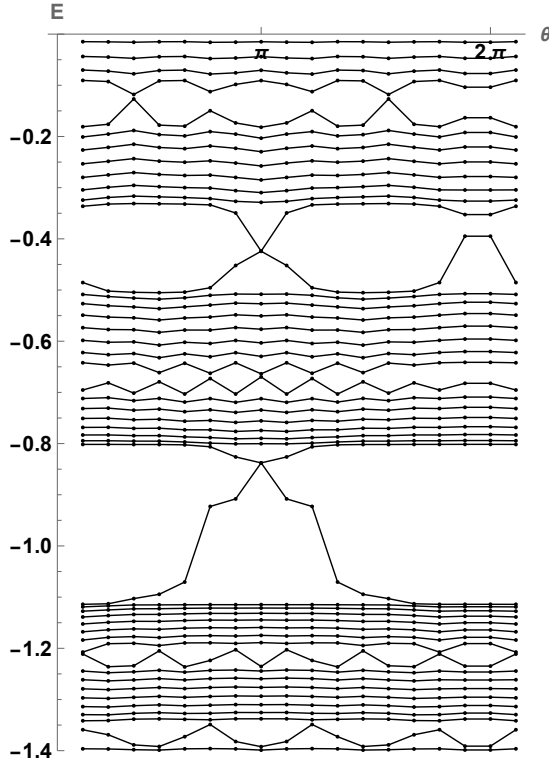


FIG. 3. Plots of the lower half of the energy spectrum of an open 1D silver mean approximant system of $N = 17$ sites, showing the evolution of energies as the phason angle θ takes 17 discrete values between 0 and 2π . Finite system of 8 unit cells was considered, with $t_A = 0.7t$, $t_B = t$. The energies E is given in units of t . The lines are only a guide to the eye, to help see the distinction between bulk states and edge states. The number of crossings of the energy of edge states in each gap can be seen to correspond to the gap label q for this $n = 2, k = 4$ approximant chain.

scheme in Eq.9. For our approximant chain, this scheme states that the j th gap labels are given by $j = 17p_j + 12q_j$ with $j = 1, \dots, 16$ such that $-N/2 \leq q_j \leq N/2$. The labels for the first 8 gaps q_j , starting from the bottom of the band are $q = -7, 3, -4, 6, -1, -8, 2$, and 5. These values correctly identify the number of periods of the motion of edge state in each of the gaps, as can be seen in Fig.3.

VI. CONCLUSIONS

Topological invariants in quasicrystals are an active subject of research, with interesting potentials applications for topologically protected states. Studies have been carried out for topological quasiperiodic systems in one and also higher dimensions. However, these studies focus on the properties of specific structures, and a global picture of topological characteristics of quasicrystals has been lacking. In this work, we have considered a family of 1D quasicrystals, and given a complete description of their topological invariants. These are the metallic mean chains, generalizations of the Fibonacci chain. We show how one can obtain the topological invariants for all of the approximants of all of the members of this family. This is done by considering their 2D parent Quantum Hall models.

The gap labelings obtained with our scheme was checked by numerical computations in finite open chains. The q indices correctly reflect the winding property of the edge states. This property has many implications for experimental systems. Edge states and their winding are interesting in many different contexts. One situation of interest occurs in models where one can induce superconducting pairing either by proximity effects [22] or electron-electron interactions [23]. Unusual Josephson effects have been predicted for the Fibonacci case [24] and should also hold for the other members of the metallic mean family.

We have shown that the spectra of metallic mean quasicrystals has a simplified Hofstadter butterfly structure. It is also interesting to note that “Landau levels” emerge in the asymptotic limit.

Although we have focused here on the pure hopping Hamiltonians, the gap labeling should apply rather generally to diagonal or mixed forms of these quasiperiodic Hamiltonians, if level crossings do not occur. More generally, the metallic mean family could provide interesting new scenarios for other coupled systems. Coupling to phonons, for

example, could lead to exotic new charge density modulated phases and topological phase transitions. Such models should be explored in future work.

[1] J. Bellissard, H. Schulz-Baldes, and A. van Elst, Noncommutative geometry of the quantum hall effect, *J. Math. Phys.* **35**, 5373 (1994).

[2] A. Panigrahi, V. Juricic, and B. Roy, Projected topological branes, *Nat. Comm. Phys.* **5**, 230 (2022).

[3] A. Jagannathan, Missing link between the two-dimensional quantum hall problem and one-dimensional quasicrystals, *Phys. Rev. B* **112**, L100102 (2025).

[4] Y. E. Kraus, Y. Lahini, Z. Ringel, M. Verbin, and O. Zilberberg, Topological states and adiabatic pumping in quasicrystals, *Phys. Rev. Lett.* **109**, 106402 (2012).

[5] Y. E. Kraus and O. Zilberberg, Topological equivalence between the fibonacci quasicrystal and the harper model, *Phys. Rev. Lett.* **109**, 116404 (2012).

[6] D. Tanese, E. Gurevich, F. Baboux, T. Jacqmin, A. Lemaître, E. Galopin, I. Sagnes, A. Amo, J. Bloch, and E. Akkermans, Fractal energy spectrum of a polariton gas in a fibonacci quasiperiodic potential, *Phys. Rev. Lett.* **112**, 146404 (2014).

[7] F. Baboux, E. Levy, A. Lemaître, C. Gómez, E. Galopin, L. Le Gratiet, I. Sagnes, A. Amo, J. Bloch, and E. Akkermans, Measuring topological invariants from generalized edge states in polaritonic quasicrystals, *Phys. Rev. B* **95**, 161114 (2017).

[8] V. Z. Cerovski, M. Schreiber, and U. Grimm, Spectral and diffusive properties of silver-mean quasicrystals in one, two, and three dimensions, *Phys. Rev. B* **72**, 054203 (2005).

[9] S. Thiem, M. Schreiber, and U. Grimm, Wave packet dynamics, ergodicity, and localization in quasiperiodic chains, *Phys. Rev. B* **80**, 214203 (2009).

[10] Thiem, S. and Schreiber, M., Generalized inverse participation numbers in metallic-mean quasiperiodic systems, *Eur. Phys. J. B* **83**, 415 (2011).

[11] J. M. Luck, A classification of critical phenomena on quasi-crystals and other aperiodic structures, *Europhysics Letters* **24**, 359 (1993).

[12] E. C. Oğuz, J. E. S. Socolar, P. J. Steinhardt, and S. Torquato, Hyperuniformity of quasicrystals, *Phys. Rev. B* **95**, 054119 (2017).

[13] M. Baake and U. Grimm, Scaling of diffraction intensities near the origin: some rigorous results, *Journal of Statistical Mechanics: Theory and Experiment* **2019**, 054003 (2019).

[14] M. Baake and U. Grimm, *Aperiodic Order* (Cambridge University Press, 2013).

[15] D. R. Hofstadter, Energy levels and wave functions of bloch electrons in rational and irrational magnetic fields, *Phys. Rev. B* **14**, 2239 (1976).

[16] A. Cerjan and T. A. Loring, Local invariants identify topology in metals and gapless systems, *Phys. Rev. B* **106**, 064109 (2022).

[17] N. Macé, A. Jagannathan, and F. Piéchon, Gap structure of 1d cut and project hamiltonians, *Journal of Physics: Conference Series* **809**, 012023 (2017).

[18] J. Bellissard, A. Bovier, and J.-M. Ghez, Discrete schrödinger operators with potentials generated by substitutions, in *Differential Equations with Applications to Mathematical Physics*, Mathematics in Science and Engineering, Vol. 192, edited by W. Ames, E. Harrell, and J. Herod (Elsevier, 1993) pp. 13–23.

[19] J. Kellendonk and E. Prodan, Bulk–Boundary Correspondence for Sturmian Kohmoto-Like Models, *Annales Henri Poincaré* [10.1007/s00023-019-00792-5](https://doi.org/10.1007/s00023-019-00792-5) (2019).

[20] A. Jagannathan, Topological connections between the 2d quantum hall problem and the 1d quasicrystal (2026), arXiv:2601.09432 [cond-mat.mes-hall].

[21] J. Kellendonk and L. Scaglione, Augmentation and bulk edge correspondence for one dimensional aperiodic tight binding operators (2026), arXiv:2512.01555 [math-ph].

[22] G. Rai, S. Haas, and A. Jagannathan, Proximity effect in a superconductor-quasicrystal hybrid ring, *Phys. Rev. B* **100**, 165121 (2019).

[23] A. Kobiałka, O. A. Awoga, M. Leijnse, T. Domański, P. Holmvall, and A. M. Black-Schaffer, Topological superconductivity in fibonacci quasicrystals, *Phys. Rev. B* **110**, 134508 (2024).

[24] I. Sardinero, J. Cayao, K. Yada, Y. Tanaka, and P. Burset, The josephson effect in fibonacci superconductors (2025), arXiv:2507.19147 [cond-mat.supr-con].